Macromolecules **2003,** *36,* 2176−2178

Notes

Study of the Dual Amorphous Phases in Semicrystalline Poly(ethylene terephthalate) Using the Heat Capacity Increment at the Glass Transition

Jun Zhao,[†] Wei Dong,[‡] Chaoxu Li,[†] Meili Guo,[‡] and Qingrong Fan*,[†]

State Key Laboratory of Polymer Physics & Chemistry,
Joint Laboratory of Polymer Science & Materials,
Center for Molecular Science, Institute of Chemistry,
Chinese Academy of Sciences, Beijing 100080, P. R. China,
and School of Materials Science & Engineering,
Beijing University of Aeronautics & Astronautics,
Beijing 100083, P. R. China

Received August 15, 2002
Revised Manuscript Received December 2, 2002

The morphology of semicrystalline polymers is increasingly interesting due to its theoretical importance,[1,2] and many models have been proposed to explain the particular properties of semicrystalline polymers.[3−9] The model of "extended glass transition" proposed by Struik[3,4] describes the amorphous phase in semicrystalline polymers as a distribution of subphases with different glass transition temperatures (T_g) and has been employed in our previous papers[10,11] to successfully explain the physical aging behaviors of semicrystalline poly(ethylene terephthalate) (PET). However, the model of "rigid amorphous phase" proposed by Wunderlich et al.[5−8] divides the amorphous phase in semicrystalline polymers into a mobile amorphous subphase, which contributes to and is proportional to the heat capacity increment (ΔC_p) at the glass transition, and a rigid amorphous subphase, which does not contribute to the ΔC_p. Besides, the concept of "rigid noncrystalline chains" proposed by Zachmann[9] separates the noncrystalline chains in semicrystalline polymers into rigid noncrystalline chains and mobile noncrystalline chains by their conformations. In the present paper, the model of "rigid amorphous phase" will be used to further study the structural changes in semicrystalline PET during isothermal crystallization from the glassy state.

Amorphous PET films had a thickness of ca. 0.15 mm, a viscosity-average molecular weight of ca. 1.63×10^4, a density of ca. 1.335 g cm^{-3}, which means that samples were wholly amorphous, and an optical birefringence of ca. 6×10^{-4}, which means that there was no orientation. Measurements by both differential scanning calorimetry (DSC) and wide-angle X-ray diffraction (WAXD) also showed that the samples were wholly amorphous.

As-received PET films were cut into equal circles with a diameter of ca. 5.7 mm. They were held in an oven under a nitrogen atmosphere at 573 ± 0.5 K (ca. 45 K above their melting point of ca. 528 K) for 5 min to completely eliminate their thermal history. Then they were quenched in air to the room temperature of ca. 298 K. It has been proved that there was no crystallization induced by this process. Subsequently, these quenched samples crystallized isothermally in an oven under a nitrogen atmosphere at various preset temperatures between 358 and 408 K for different periods of time to obtain a different degree of crystallinity (X_c). Finally, all the semicrystalline samples were taken out and stored in a desiccator before other measurements.

The density of semicrystalline PET (ρ) was measured at 298 ± 0.1 K by using a density gradient tube filled with carbon tetrachloride and *n*-heptane. The density gradient tube was calibrated by suspending glass beads with known densities. X_c (apparent weight percent degree of crystallinity) of the samples was calculated by taking the density of wholly amorphous samples (ρ_a) to be 1.335 g cm^{-3} and that of perfect PET crystalline lamellae (ρ_c) to be 1.455 g cm^{-3}.[12] Then

$$X_c\,(\%) = (\rho_c(\rho - \rho_a))/(\rho(\rho_c - \rho_a)) \times 100 \qquad (1)$$

Samples of ca. 5.0 mg were sealed in aluminum pans, and their thermal properties were measured by using a TA2910 DSC. Indium and tin were employed for the temperature calibration, the heat capacity was evaluated with respect to sapphire as a standard, and a nitrogen gas purge with a flux of ca. 30 mL min^{-1} was used to prevent oxidative degradation of samples during the heating run. The rate of heating run in DSC was 10 K min^{-1}.

According to the model of "rigid amorphous phase",[5−8] the fraction of the mobile amorphous phase (X_{ma}) was calculated directly from the ΔC_p at the glass transition. For all the semicrystalline samples, a perfect heat capacity step without any endothermic peak was obtained, and the T_g was measured at half-devitrification.[5−8] Our experimental results showed that the ΔC_p of wholly amorphous samples was ca. 0.410 J g^{-1} K^{-1}, which was consistent with another report.[13] Then

$$X_{ma}\,(\%) = \Delta C_p/0.410 \times 100 \quad \text{(refs 5−8)} \qquad (2)$$

and the fraction of the rigid amorphous phase (X_{ra}) could be obtained

$$X_{ra}\,(\%) = 100 - X_c - X_{ma} \quad \text{(refs 5−8)} \qquad (3)$$

Figure 1 presents the evolution laws of X_c, X_{ma}, and X_{ra} with increasing t_c for isothermal crystallization from the glassy state at 373, 388, and 403 K, respectively. From Figure 1a, it can be seen that X_c increased with increasing logarithm of crystallization time (t_c) and

---

[†] Chinese Academy of Sciences.

[‡] Beijing University of Aeronautics & Astronautics.

* To whom correspondence should be addressed: Tel +86 10 82618124; Fax +86 10 62559373; e-mail qrfan@pplas.icas.ac.cn.

10.1021/ma021331u CCC: $25.00

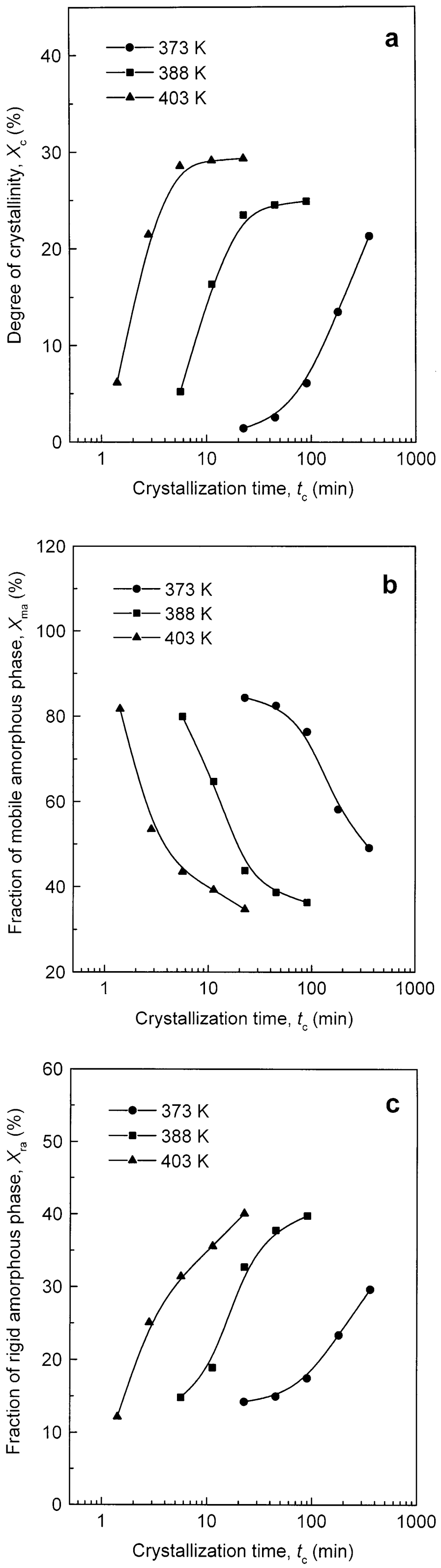

Figure 1. Evolution of X_c (a), X_{ma} (b), and X_{ra} (c) with increasing t_c for isothermal crystallization from the glassy state at 373, 388, and 403 K, respectively.

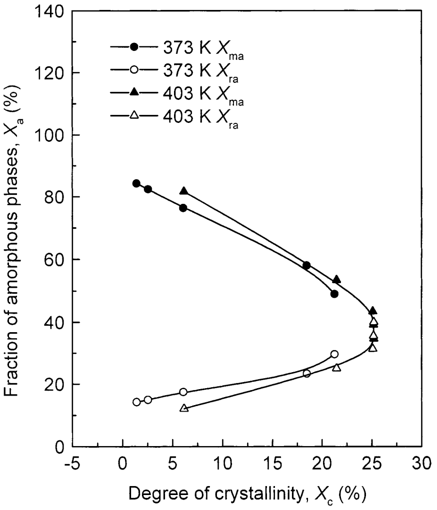

Figure 2. Evolution of X_{ma} and X_{ra} with increasing X_c for isothermal crystallization from the glassy state at 373 and 403 K, respectively (measured from Figure 1).

showed a sigmoid shape, which has been well documented. For the same t_c, X_c was higher for higher crystallization temperature (T_c), which suggests that the crystallization rate increased with increasing T_c in this temperature range. From Figure 1b, it can be seen that X_{ma} decreased with increasing logarithm of t_c and showed an antisigmoid shape. For the same t_c, X_{ma} was lower for higher T_c, which suggests that the decrease rate of X_{ma} increased with increasing T_c. From Figure 1c, it can be seen that X_{ra} increased with increasing logarithm of t_c and also showed a sigmoid shape. For the same t_c, X_{ra} was higher for higher T_c. It is interesting to notice that X_{ra} was calculated from X_c and X_{ma} by eq 3. As a matter of fact, our experimental results showed that other T_c between 358 and 408 K also followed such evolution laws of both X_{ma} and X_{ra}.

By combining parts a–c of Figure 1, it can be seen that, during the isothermal crystallization, coupled with the increase of X_c, X_{ma} decreased while X_{ra} increased. That is to say, both the crystallites and the rigid amorphous phase formed at the cost of the mobile amorphous phase. Our experimental results also showed that, coupled with such structural changes, the T_g of semicrystalline samples increased with increasing t_c.

Figure 2 presents the evolution laws of X_{ma} and X_{ra} with increasing X_c for isothermal crystallization from the glassy state at 373 and 403 K, respectively. It can be seen that X_{ma} decreased while X_{ra} increased with increasing X_c. This is consistent with another report,[8] but it is not a common phenomenon in semicrystalline polymers since in some other semicrystalline polymers both X_{ma} and X_{ra} were found to decrease with increasing X_c.[7,14,15] It is interesting to find that for the T_c of 403 K, when X_c had reached a constant value, X_{ma} continued to decrease while X_{ra} continued to increase. This is a direct observation of evolution of the mobile amorphous phase into the rigid amorphous phase. From Figure 2, a more interesting result also can be obtained that, for the same X_c, X_{ma} increased while X_{ra} decreased with increasing T_c, which suggests that higher T_c favored the formation of mobile amorphous phase. Such experimental results are consistent with our previous report[11] that higher T_c favored the formation of an amorphous subphase with higher segmental mobility. As a matter of fact, our experiments showed that such laws worked in the whole T_c range between 358 and 408 K.

Acknowledgment. This work was subsidized by the Special Funds for Major State Basic Research Projects (95-12 and G1999064800).

References and Notes

(1) Read, B. E.; Tomlins, P. E.; Dean, G. D. *Polymer* **1990**, *31*, 1204−1215.

(2) Diego, J. A.; Canadas, J. C.; Mudarra, M.; Belana, J. *Polymer* **1999**, *40*, 5355−5363.

(3) Struik, L. C. E. *Physical Aging in Amorphous Polymers and Other Materials*; Elsevier: Amsterdam, 1978.

(4) Struik, L. C. E. *Polymer* **1987**, *28*, 1521−1533, 1534−1542; **1989**, *30*, 799−814, 815−830.

(5) Cheng, S. Z. D.; Cao, M.-Y.; Wunderlich, B. *Macromolecules* **1986**, *19*, 1868−1876.

(6) Cheng, S. Z. D.; Wu, Z. Q.; Wunderlich, B. *Macromolecules* **1987**, *20*, 2802−2810.

(7) Cheng, S. Z. D.; Heberer, D. P.; Lien, H.-S.; Harris, F. W. *J. Polym. Sci., Polym. Phys.* **1990**, *28*, 655−674.

(8) Chalmers, T. M.; Zhang, A.; Shen, D.; Lien, S. H.-S.; Tso, C. C.; Gabori, P. A.; Harris, F. W.; Cheng, S. Z. D. *Polym. Int.* **1993**, *31*, 261−268.

(9) Zachmann, H. G. *Polym. Eng. Sci.* **1979**, *19*, 966−974.

(10) Zhao, J.; Song, R.; Zhang, Z.; Linghu, X.; Zheng, Z.; Fan, Q. *Macromolecules* **2001**, *34*, 343−345.

(11) Zhao, J.; Wang, J.; Li, C.; Fan, Q. *Macromolecules* **2002**, *35*, 3097−3103.

(12) Vigier, G.; Tatibouet, J.; Benatmane, A.; Vassoille, R. *Colloid Polym. Sci.* **1992**, *270*, 1182−1187.

(13) Okazaki, I.; Wunderlich, B. *J. Polym. Sci., Polym. Phys.* **1996**, *34*, 2941−2952.

(14) Coburn, J. C.; Boyd, R. H. *Macromolecules* **1986**, *19*, 2238−2245.

(15) Huo, P.; Cebe, P. *Macromolecules* **1992**, *25*, 902−909.

MA021331U